

First Measurement of the Reaction ${}^3\text{He}(\vec{\gamma}, p)X$ with Polarized Photons

C. Ruth,³ G. S. Adams,³ H. Baghaei,⁸ A. Caracappa,¹ W. B. Clayton,³ A. D'Angelo,⁴ M.-A. Duval,^{6,*} G. Giordano,² S. Hoblit,⁸ O. C. Kistner,¹ J. M. Laget,⁹ R. Lindgren,⁸ G. Matone,² L. Miceli,¹ W. K. Mize,⁶ M. A. Moinester,⁷ A. M. Sandorfi,¹ C. Schaerf,⁴ R. M. Sealock,⁸ L. C. Smith,⁸ P. Stoler,³ D. J. Tedeschi,³ P. K. Teng,^{3,5} C. E. Thorn,¹ S. T. Thornton,⁸ K. Vaziri,^{3,†} C. S. Whisnant,^{1,6} and E. J. Winhold³

¹Physics Department, Brookhaven National Laboratory, Upton, New York 11973

²Istituto Nazionale di Fisica Nucleare-Laboratori Nazionali di Frascati, Frascati, Italy

³Physics Department, Rensselaer Polytechnic Institute, Troy, New York 12180-3590

⁴Istituto Nazionale di Fisica Nucleare and University of Rome Tor Vergata, Via della Ricerca Scientifica, 00133 Rome, Italy

⁵Institute of Physics, Academia Sinica, Taipei, Republic of China

⁶Department of Physics, University of South Carolina, Columbia, South Carolina 29208

⁷School of Physics and Astronomy, Tel-Aviv University, 69978 Tel-Aviv, Israel

⁸Physics Department, University of Virginia, Charlottesville, Virginia 22903

⁹Département de Physique Nucléaire/Service de Physique Nucléaire, CE Saclay, 91191 Gif-sur-Yvette, Cedex, France
(Received 9 August 1993)

The first measurement of the reaction ${}^3\text{He}(\vec{\gamma}, p)X$ using linearly polarized photons is reported. Cross sections and beam-polarization asymmetries for $\theta_p^{\text{lab}} = 60^\circ - 100^\circ$ and $E_\gamma = 195 - 304$ MeV are compared with a microscopic calculation which includes one-, two-, and three-nucleon absorption mechanisms. One- and two-nucleon absorption alone fails to describe the data at low proton momenta. The inclusion of three-nucleon absorption significantly improves the comparison with the measured cross sections. However, some features of the asymmetry distributions are not explained.

PACS numbers: 25.20.-x, 24.70.+s, 25.10.+s

Intermediate energy photons are an excellent probe of mesonic and nucleonic currents in nuclear reactions. Photons easily couple to the low mass mesons and baryons but without the significant distortions experienced by hadronic probes. The dominant channels for photon absorption at a few hundred MeV are quasifree pion production, and absorption on a correlated p - n pair (quasideuteron). The latter reaction results in a distinctive peak at high momentum in the inclusive proton spectrum from ${}^3\text{He}$ [1] and other light nuclei [2-5].

The study of photon absorption on ${}^3\text{He}$ allows one to examine specific mechanisms on a microscopic level since realistic nuclear wave functions exist [6] and final state interactions can be explicitly treated in a multiple scattering approach [7,8]. Recent measurements suggest that three-nucleon mechanisms play a significant role in photon [9-11] and pion [12-18] absorption on ${}^3\text{He}$. The function of these multinucleon mechanisms has not been fully established for the inclusive reaction ${}^3\text{He}(\gamma, p)X$.

Polarization observables offer a more stringent test of theory than the differential cross sections alone, although they have seldom been measured in photonuclear reactions. The only previous measurements [19,20] using polarized photons on ${}^3\text{He}$ were for the two-body breakup reaction ${}^3\text{He}(\vec{\gamma}, p)d$. The present experiment is the first to measure the reaction ${}^3\text{He}(\vec{\gamma}, p)X$ with polarized photons. It covered a broad range of kinematics including regions where three-nucleon absorption mechanisms are expected to dominate [21].

The experiment was performed at the Laser Electron Gamma Source (LEGS) located at the National Syn-

chrotron Light Source at Brookhaven National Laboratory. The photon beam was produced by backscattering linearly polarized ultraviolet laser light from a 2.5 GeV electron beam. The struck electrons were momentum analyzed in a tagging spectrometer which determined the associated photon energy with a resolution of about 5 MeV (FWHM). Details of the LEGS facility can be found in Ref. [22]. The photon energy spectrum was approximately flat, extending from 195 MeV up to the Compton edge at 304 MeV. The γ -ray polarization, which ranged from 73% at 200 MeV to 99% at 304 MeV, was calculated from the measured laser polarization. The polarization was flipped randomly between states parallel (\parallel) and perpendicular (\perp) to the γ -proton reaction plane, in order to reduce the systematic uncertainty. The liquid ${}^3\text{He}$ target was cylindrical with a length of 10 cm along the beam direction, and a 5 cm diameter. The target cell was made by electroforming Ni to a thickness of 0.01 cm. Electron-positron pair production counters were used to monitor the photon flux downstream of the target. Protons were detected in 24 CaF_2 /plastic scintillator telescopes arranged in eight groups of three with $20^\circ \leq \theta_p^{\text{lab}} \leq 160^\circ$. These detectors consisted of a thin (0.1-0.2 cm) CaF_2 , ΔE detector, coupled to a thick (30-50 cm) plastic, E detector. Particle identification was accomplished with cuts on the correlated ΔE and E signals. The resulting proton energy resolution was typically 6% (FWHM).

We present the results at selected angles which show the salient features of the data. The complete data set will be published in a forthcoming paper. The unpolar-

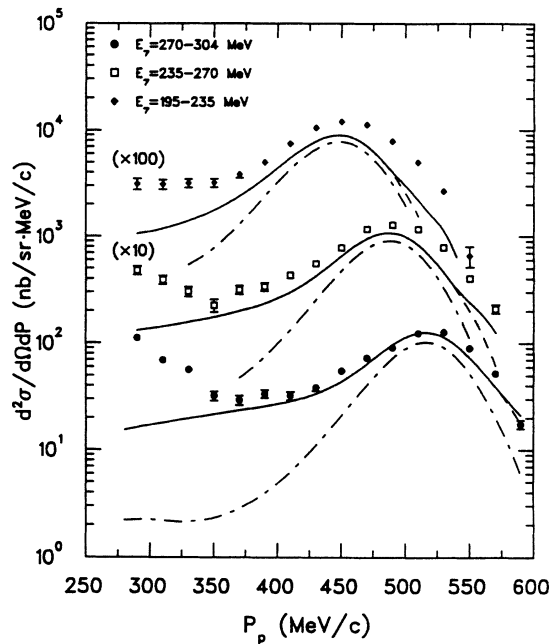


FIG. 1. Cross section at $\theta_p=80^\circ$ for three E_γ cuts. The dash-dotted curve includes $1N+2N$ absorption, the dashed curve is the sum of $1N+2N+3N$, and the solid curve is the sum of the dashed curve plus p - d breakup of ${}^3\text{He}$. The solid and dashed curves are indistinguishable over most of the momentum range.

ized differential cross section measured at 80° is shown in Fig. 1 for three photon energy cuts which span the full range of the measurement. The error bars shown are statistical only. The systematic error is estimated to be $\pm 5\%$, with the major contributions coming from the uncertainties in the $\vec{\gamma}$ flux and detector solid angle. Figure 2 shows the beam polarization asymmetry data for $E_\gamma=270$ - 304 MeV, at 60° , 80° , and 100° . Here the asymmetry is defined as $\Sigma=(d\sigma_{\parallel}-d\sigma_{\perp})/(d\sigma_{\parallel}+d\sigma_{\perp})$.

It is useful to describe the data in terms of three regions. The prominent peak in the cross section at high momentum is primarily due to absorption on a correlated pn pair. This peak also contains a small contribution from the two-body breakup channel, ${}^3\text{He}(\vec{\gamma},p)d$, which is not resolved from the three-nucleon final state. The rise in the cross section at low momentum which can be seen at photon energies $E_\gamma=235$ - 304 MeV is consistent with what one expects from quasifree π production, where the recoiling proton is detected. In Fig. 1 the low momentum side of the quasifree peak is cut off by the detector threshold, which limits the measured spectrum to $P_p \geq 270$ MeV/c. The third region lies between the quasideuteron and π production regions. This is the best place to observe the effect of the three-nucleon absorption mechanisms. These mechanisms have been predicted to dominate the breakup reaction below the quasideuteron peak [21].

The present data are compared with the results of a

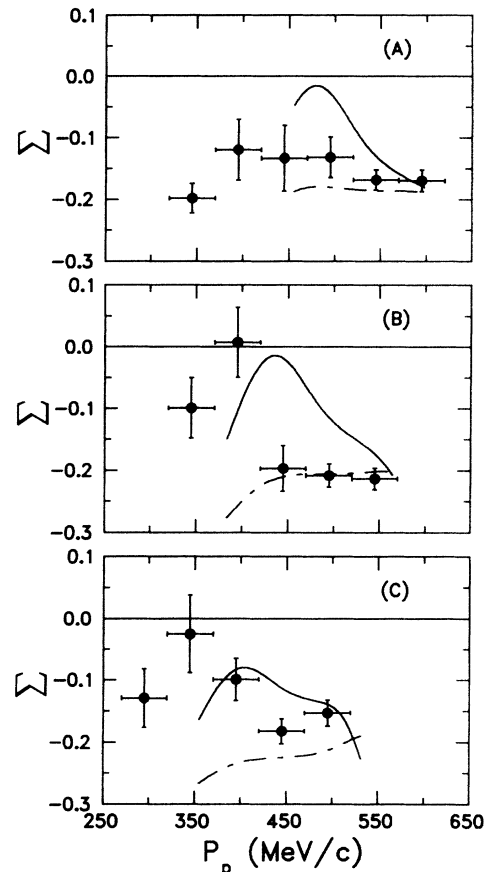


FIG. 2. Photon asymmetry, $\Sigma=(d\sigma_{\parallel}-d\sigma_{\perp})/(d\sigma_{\parallel}+d\sigma_{\perp})$, for $E_\gamma=270$ - 304 MeV at (a) 60° , (b) 80° , and (c) 100° . The dash-dotted curve includes $1N+2N$ absorption and the solid curve is the result when $1N+2N+3N$ amplitudes are added together.

microscopic calculation which includes the meson exchange mechanisms depicted in Fig. 3. Nucleon-nucleon final state interactions (not shown in the diagrams) were included by parametrizing the off-shell amplitudes in terms of the half-off-shell solutions of the two body scattering equation for the Reid potential. Partial waves up to $L=2$ were included. The bound state ${}^3\text{He}$ wave function is a solution of the Faddeev equations for the Reid potential. It should be noted that since the N - N final state interactions are treated perturbatively (as a truncated scattering series), the final state wave functions are not eigenstates of the three-nucleon Hamiltonian from which the ground state is derived. Details of the calculation have been reported previously [7,23]. The dash-dotted curve in Fig. 1 is the result of the calculation including the one- and two-nucleon ($1N+2N$) absorption diagrams, Figs. 3(a) and 3(b). The dashed curve shows the result when the three-nucleon ($3N$) absorption diagrams [Fig. 3(c)] are included. The $3N$ amplitudes are maximized when the photoproduced pion is on-shell and is subsequently absorbed by a $T=0$, n - p pair. The full

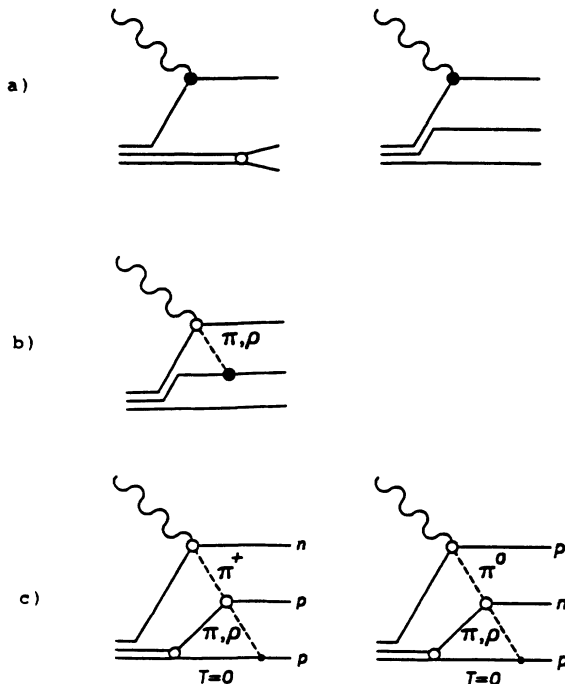


FIG. 3. Diagrams that are included in the calculation. (a) is $1N$ absorption, (b) is $2N$ absorption, and (c) is $3N$ absorption with pion rescattering.

curve contains the additional contribution of the two-body breakup reaction, which is not resolved from three-body breakup in the present data. This contribution can be seen at the highest momenta as the difference between the dashed and solid curves. It was empirically added by fitting the angular distribution measurements of Gassen *et al.* [24] for $\gamma^3\text{He} \rightarrow pd$ and folding with the experimental resolution. The data in Ref. [24] were scaled by a factor of 1.39 to bring them into agreement with the measurement of Sober *et al.* [25] and with the data from the inverse reaction [26] before fitting. All theoretical results were averaged over the experimental photon energy distribution and proton momentum bin widths.

From the comparison with the theoretical predictions (dashed-dotted curve in Fig. 1) it is evident that the peak in the differential cross section at high momentum is dominated by $2N$ absorption. The $1N$ contribution is small due to the large mismatch between the photon and nucleon momenta. However, the $1N+2N$ results lie far below the measured strength at proton momenta below the quasideuteron peak. It is in this region that the addition of $3N$ amplitudes (dashed and solid curves) have a profound effect. For the highest E_γ cut, the full theory is in excellent agreement with the data for $P_p \geq 400$ MeV/c. (The calculations for lower momenta underestimate the data, but this is to be expected since the model does not include real-pion production channels.) For $E_\gamma = 270\text{--}304$ MeV the integrated theoretical cross section increases by a factor of 1.75 when $3N$ amplitudes are

included. At lower photon energies the effects due to the $3N$ amplitudes remain quite significant, although the calculations underestimate the measured cross sections. Similar discrepancies were observed when the elementary deuteron photodisintegration cross section was calculated [27].

The comparisons between the present data and theory, at 80° (Fig. 1) and other angles, support the predictions [1,21] that $2N$ and $3N$ absorption dominate the reaction $^3\text{He}(\gamma, p)X$ at different proton momenta. The beam polarization asymmetry, Σ , which is the ratio of the difference of contributions from orthogonal polarization states to the unpolarized cross section, provides an important independent test of this model. For the $2N$ process the same model is able to account for the observed asymmetries in deuteron photodisintegration, while much smaller asymmetries are expected when three nucleons share the incident beam energy.

The predicted asymmetries for $E_\gamma = 270\text{--}304$ MeV are shown in Fig. 2. Theory gives the best description of the measured cross sections in this energy range. The asymmetry data, as well as the calculations using $1N+2N$ amplitudes (dashed-dotted lines), lie close to the deuteron values [28] (approximately -0.20) at high momentum. This agrees with our previous interpretation of the quasideuteron region. The addition of $3N$ amplitudes (solid curves) causes the predicted asymmetries to rise smoothly toward zero with decreasing momentum. However, the data do not consistently follow the predictions, with some angles being worse than others. In particular, at 60 and 80 degrees the asymmetries remain below the solid curves, at essentially the quasideuteron values, through much of the region that the analyses of the unpolarized data had ascribed to the $3N$ absorption mechanism. At lower beam energies the discrepancies are generally less, but the effect of the $3N$ amplitudes is also reduced.

In summary, inclusive protons have been measured from the reaction $^3\text{He}(\vec{\gamma}, p)X$ using polarized photon beams. One- and two-nucleon absorption mechanisms alone fall far short of accounting for the measured cross sections below the quasideuteron peak. The inclusion of three-nucleon amplitudes has a large effect and is clearly important. However, the present state of the theory provides at best an incomplete description of the cross sections and beam asymmetries. One possible improvement of the theory which could significantly alter the asymmetries is the treatment of final state interactions. At low energies the spin observables for radiative proton capture on deuterium are dramatically improved in a theory which generates bound and continuum states from the same nuclear Hamiltonian [29].

This work was supported in part by the U.S. Department of Energy under Contract No. DE-AC02-76-CH00016, the National Science Foundation, the Istituto Nazionale di Fisica Nucleare, and the U.S.-Israel Binational Science Foundation.

- *Present address: Institute de Physique Nucleaire, 91406 Orsay, Cedex, France.
- †Present address: Fermilab, MS 119 ES&H, Box 500, Batavia, IL 60510.
- [1] N. d'Hose *et al.*, Phys. Rev. Lett. **63**, 856 (1989).
- [2] M. Kanazawa *et al.*, Phys. Rev. C **35**, 1828 (1987).
- [3] S. Homma *et al.*, Phys. Rev. C **36**, 1623 (1987).
- [4] S. Hamma *et al.*, Phys. Rev. Lett. **45**, 706 (1980).
- [5] J. Arends *et al.*, Z. Phys. A **298**, 103 (1980).
- [6] J. L. Friar, in *Modern Topics in Electron Scattering*, edited by B. Frois and I. Sick (World Scientific, Singapore, 1991), pp. 104–136.
- [7] J. M. Laget, Phys. Lett. **151B**, 325 (1985).
- [8] J. M. Laget, Phys. Rev. C **35**, 832 (1986).
- [9] G. Audit *et al.*, Phys. Lett. B **227**, 331 (1989).
- [10] G. Audit *et al.*, Phys. Rev. C **44**, R575 (1991).
- [11] A. J. Sarty *et al.*, Phys. Rev. C **47**, 459 (1993).
- [12] K. A. Aniol *et al.*, Phys. Rev. C **33**, 1714 (1986).
- [13] S. Mukhopadhyay *et al.*, Phys. Rev. C **43**, 957 (1991).
- [14] P. Weber *et al.*, Nucl. Phys. A **534**, 541 (1991).
- [15] G. Backenstoss *et al.*, Phys. Lett. B **222**, 7 (1989).
- [16] G. Backenstoss *et al.*, Phys. Rev. Lett. **25**, 2782 (1985).
- [17] C. Smith *et al.*, Phys. Rev. C **40**, 1347 (1989).
- [18] S. MayTal-Beck *et al.*, Phys. Rev. Lett. **68**, 3012 (1992).
- [19] A. A. Belyaev *et al.*, Yad. Fiz. **44**, 289 (1986) [Sov. J. Nucl. Phys. **44**, 181 (1986)].
- [20] F. L. Fabbri *et al.*, Nuovo Cimento Lett. **3**, 63 (1972).
- [21] J. M. Laget, Nucl. Phys. A **497**, 391 (1989).
- [22] C. E. Thorn *et al.*, Nucl. Instrum. Methods Phys. Res., Sect. A **285**, 447 (1989); W. K. Mize, Ph.D. thesis, University of South Carolina, 1992.
- [23] J. M. Laget, J. Phys. G **14**, 1445 (1988).
- [24] H. J. Gassen *et al.*, Z. Phys. A **303**, 35 (1981).
- [25] D. I. Sober *et al.*, Phys. Rev. C **28**, 2234 (1983).
- [26] W. J. Briscoe *et al.*, Phys. Rev. C **32**, 1956 (1985).
- [27] J. M. Laget, Can. J. Phys. **62**, 1046 (1984).
- [28] L. Micheli *et al.*, in Proceedings of the Particles and Nuclei International Conference, Perugia, Italy, June 1993 (unpublished).
- [29] A. C. Fonseca and D. R. Lehman, Phys. Rev. C **48**, R503 (1993), and references therein.